

FLane: An Adaptive Fuzzy Logic Lane Tracking System for Driver Assistance

Giulio Reina¹

Department of Engineering for Innovation,
University of Salento,
Via per Arnesano,
73100 Lecce, Italy
e-mail: giulio.reina@unisalento.it

Annalisa Milella

Institute of Intelligent Systems for Automation,
National Research Council,
Via G. Amendola 122/D,
70126 Bari, Italy
e-mail: milella@ba.issia.cnr.it

In the last few years, driver assistance systems are increasingly being investigated in the automotive field to provide a higher degree of safety and comfort. Lane position determination plays a critical role toward the development of autonomous and computer-aided driving. This paper presents an accurate and robust method for detecting road markings with applications to autonomous vehicles and driver support. Much like other lane detection systems, ours is based on computer vision and Hough transform. The proposed approach, however, is unique in that it uses fuzzy reasoning to combine adaptively geometrical and intensity information of the scene in order to handle varying driving and environmental conditions. Since our system uses fuzzy logic operations for lane detection and tracking, we call it "FLane." This paper also presents a method for building the initial lane model in real time, during vehicle motion, and without any a priori information. Details of the main components of the FLane system are presented along with experimental results obtained in the field under different lighting and road conditions.
[DOI: 10.1115/1.4003091]

1 Introduction

Within the last few years, research into intelligent vehicles has greatly expanded. Systems that monitor driver intent, warn drivers of lane departure, or provide vehicle assistance are all emerging. Specifically, lane detection and tracking is a well-researched problem in computer vision with a wide range of applications in autonomous vehicles and driver support systems. Lane detection can be employed in the following driver assistance applications [1]:

- *Lane-departure-warning system.* The system predicts the trajectory of the vehicle with respect to the lane boundary [2] (Fig. 1(a)).
- *Driver-attention monitoring system.* The system monitors the driver's attentiveness to the lane-keeping task using parameters such as the smoothness of the lane following [3] (Fig. 1(b)).
- *Automated vehicle-control system.* The system automatically guides safely the vehicle within the lane by controlling the lateral position error [4] (Fig. 1(c)).

Finding white markings on a dark road can turn into a very complex problem when shadows, physical barriers, occlusions by other vehicles, changes in road surfaces, and different types of lane markings come into play. A robust and efficient lane detection system must be able to filter out all disturbances and extract the markings of interest from cluttered roadways in order to produce an accurate and reliable estimate of the vehicle position relative to the road. In Fig. 2, a sample image set demonstrates the variety of road and environmental conditions that can be encountered. Figure 2(a) shows a scene where lane detection can be considered relatively easy thanks to a clearly defined, solid marking and a uniform road texture. In Fig. 2(b), extraction of road marking is more difficult due to the presence of a curb and a manhole cover. Figure 2(c) shows a more complex road marking with transversal solid lines due to side road enters, while in Fig.

2(d) a nonuniform road texture is shown. Finally, Figs. 2(e) and 2(f) refer to low lighting scenes due to overpasses and night time.

Many researchers have developed lane detectors based on various techniques. A commonly used approach is the Hough transform, which fits lines to detected edges [5,6]. This approach typically suffers from heavy computational requirements that make it a difficult real-time implementation and can easily fail in situations where many extraneous lines exist. Neural networks have been used to attempt to detect lanes and control vehicles [7] but have difficulties on roads not included in their training set. Techniques using tangent vectors have also been demonstrated to be quite robust on well-marked roads but can fail when lane markings are not well-defined [8]. Other researchers have attempted to overcome problems of differing lane markings by using multiple detectors. For example, Gehrig et al. [9] detected bots dots on California highways using specific matched filters and detected solid lane markings using more classical methods. Others, such as the authors of Refs. [10–12], proposed the use of particle filtering to improve robustness to lighting and road changes, while Bertozzi and Broggi [13] developed the generic obstacle and lane detection (GOLD) system for robust obstacle and lane detection. McCall and Trivedi [14] used steerable filters for accurate and robust lane marking detection. Frequency-based techniques, such as the lane-finding in ANother domAin (LANA) system [15], have been shown to be effective in dealing with extraneous edges. Other techniques, such as the rapidly adapting lateral position handler (RALPH) system [16], based the lane position on an adaptive road template. Such techniques generally assume a constant road surface texture and can fail in situations like the one in Fig. 2(d). While these methods are all very effective at performing lane detection in several contexts, they tend to be highly influenced by the road type or conditions. Robust lane detection remains, therefore, an open research area, since, in order to have a robust lane detector, the system must be invariant to different road markings, road conditions, lighting changes, shadowing, and occlusions.

In this paper, we investigate an alternative method based on a Hough transform enhanced by fuzzy reasoning to provide a real-time, robust, and accurate lane detection and tracking system in highly dynamic environments. Fuzzy logic allows one to cope with complex dynamical contexts that are difficult to model with mathematical approaches [17,18]. A few authors have proposed

¹Corresponding author.

Contributed by the Dynamic Systems Division of ASME for publication in the JOURNAL OF DYNAMIC SYSTEMS, MEASUREMENT, AND CONTROL. Manuscript received July 9, 2008; final manuscript received: July 23, 2010; published online February 11, 2011. Assoc. Editor: Marcio de Queiroz.

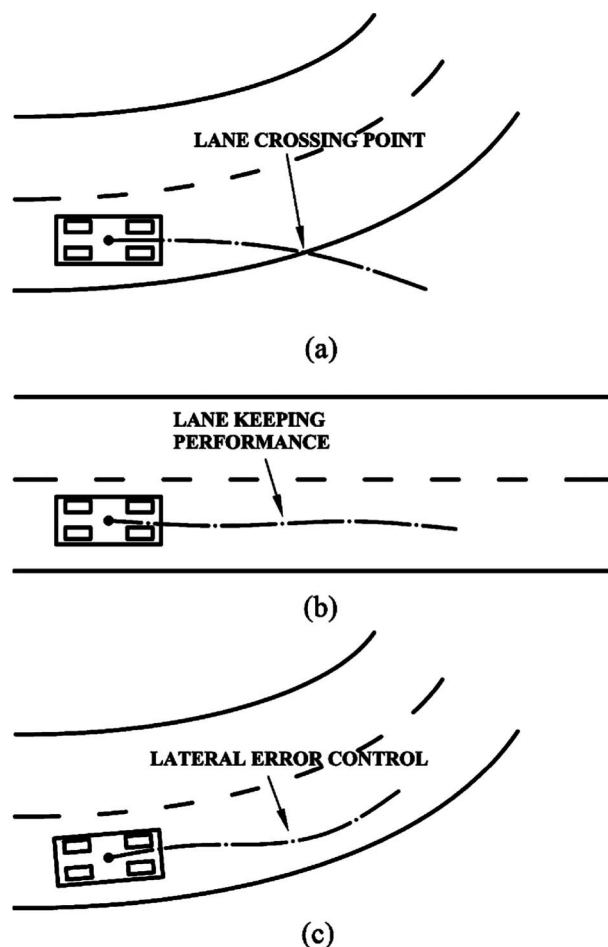


Fig. 1 Driver assistance systems that require lane position: (a) lane-departure warning, (b) driver-attention monitoring, and (c) vehicle-control

fuzzy systems in the context of lane detection in order to improve specific functions, such as edge detection [19,20]. Here, instead, fuzzy logic serves as a general framework to deal with the whole process of lane detection and tracking. Although lane detection systems have been extensively studied, one commonly-recognized issue is the lack of uniform performance characterization methodologies [1]. Several metrics have been proposed but they all tend to be very specific. In addition, most proposed algorithms have shown limited numerical results or sample images to demonstrate the performance of the algorithms, thus making a quantitative comparison across different classes of algorithms very difficult. In this paper, we evaluate the entire vision-based algorithm for lane tracking by measuring the occurrence rate of false positives, false negatives, and misidentifications.

A key issue of lane detection systems is that of defining an adequate model for the lane marking to be tracked over subsequent images. This is particularly challenging at the start of the vehicle motion, when no prior information is available, and whenever the system fails and starts over. In this respect, the FLane system features a special module, referred to as dynamic model building (DMB). The DMB module provides online lane model construction by processing a short sequence of images using what we call the cumulative Hough matrix (CHM) in conjunction with fuzzy logic operations.

Extensive testing of the proposed approach is performed with a commercial automobile equipped with a low cost webcam and operating under different driving and environmental conditions. The results demonstrate that fuzzy reasoning is a proper framework to operate under uncertainty in visual data for lane detection and drive monitoring applications. Theoretical details of the FLane method and its modules are provided in Sec. 2. Experimental results to validate this approach and assess the system performance are presented in Sec. 3. Finally, Sec. 4 concludes this paper.

2 The FLane System

The FLane module performs its task using a robust Hough transform, enhanced by fuzzy logic operations, which provide the system with the ability to adapt rapidly to varying operational conditions. In this section, a theoretical analysis of the method is presented, also providing experimental evidences of its effectiveness in the field.

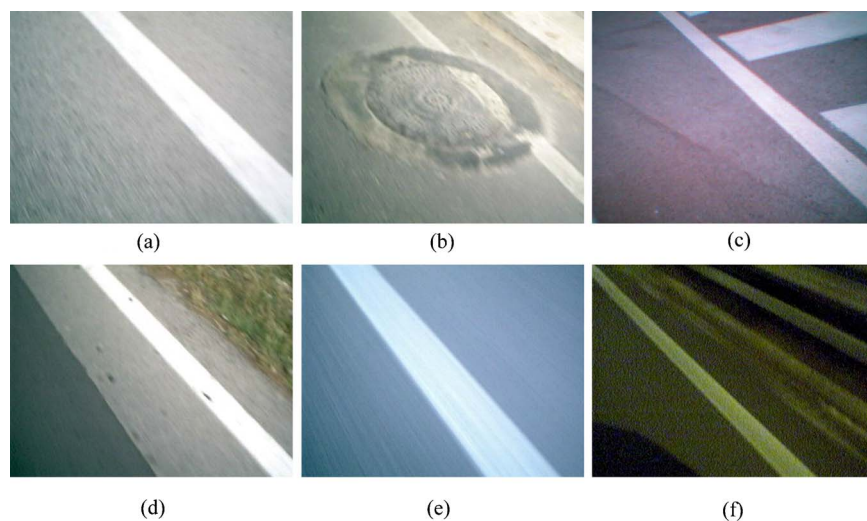


Fig. 2 Sample images of road markings and conditions: (a) simple road with solid lane marking, (b) disturbances due to curb and manhole cover, (c) transversal solid lines due to side road enters, (d) nonuniform pavement texture, (e) freeway overpass causing lighting change and reducing road-marking contrast, and (f) low lighting and shadowing at night time

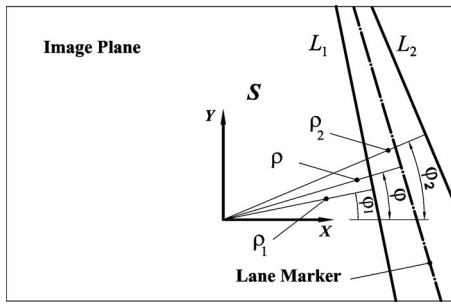


Fig. 3 Model of the lane marking in the image plane. Note that the parameters ρ_1 , ρ_2 , and ρ are expressed in pixels.

2.1 Lane Model. The presence of a sideward-facing camera mounted on the vehicle body with a field of view on the ground plane corresponding to a 90 cm long \times 120 cm wide area is assumed. It is also considered that the location of the camera relative to the ground is known and fixed during travel. Although this assumption is of limited validity since a car's suspension system allows body tilting, in a previous work [21], this approach was proved to be rather robust to relatively small changes in the position and orientation of the camera with respect to the ground. Under the further assumption that the portion of the lane marking (LM) in the image is relatively small, the lane marking curvature can be neglected, and it is possible to refer to a lane model composed of a pair of parallel lines with constant offset. In the image reference frame S , denoted with $P_1=(\rho_1, \varphi_1)$ and $P_2=(\rho_2, \varphi_2)$, the polar parameters of these two lines, namely L_1 and L_2 as explained in Fig. 3, the pose $P=(\rho, \varphi)$ of the LM model can be defined as

$$\rho = \frac{\rho_1 + \rho_2}{2} \quad (1)$$

$$\varphi = \frac{\varphi_1 + \varphi_2}{2} \quad (2)$$

In addition, the lane marker is characterized by an intensity level I_m , which is defined as the average gray level of the pixels comprised between the lane marker borders. Real world information can be obtained with good accuracy from image data by inverse perspective projection techniques, and the LM model can be defined in the real world (Fig. 4) by the following parameters

- the absolute value of the relative angle between the borders L_{1w} and L_{2w}

$$\theta = |\theta_1 - \theta_2| \quad (3)$$

θ_1 and θ_2 being the orientation of the vehicle with respect to L_{1w} and L_{2w} , respectively;

- the absolute value of the width W of the marker, which is equal to

$$W = |d_1 - d_2| \quad (4)$$

d_1 and d_2 being the minimum distance of the vehicle relative to L_{1w} and L_{2w} , respectively.

The variation range for both θ and W can be considered known by road legislation. This turns into two constraints that can be exploited for lane detection, i.e.,

$$\theta = \hat{\theta} \quad (5)$$

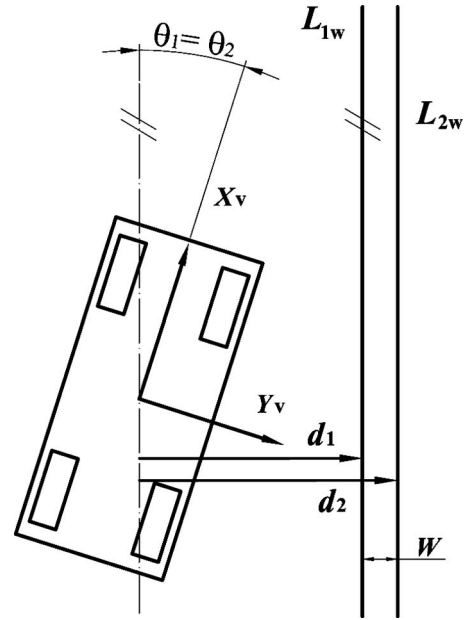


Fig. 4 Model of the lane marking in the real world. Note that the distances d_1 and d_2 are expressed in millimeters.

$$W = \hat{W} \quad (6)$$

Note that $\hat{\theta}$ is null, being the lines forming the marker parallel, and \hat{W} ranges approximately between 150 mm and 200 mm, depending on road type.

2.2 Lane Tracking. The FLane system is composed of two main submodules:

- 1) *The fuzzy edge detection (FED) module.* This module provides an intelligent fuzzy binarization of the image that allows the classical Hough transform to be applied with a substantially reduced computational requirement and a more robust and accurate implementation.
- 2) *The fuzzy lane recognition (FLR) module.* This module recognizes, between the lines extracted from the image, those lines that best fit to the lane marking model. The selection is performed by combining geometrical and intensity data of the image through fuzzy reasoning.

It should be noted that the FLane system updates the reference lane at each new acquisition. One critical aspect connected with this approach lies in building the initial model and updating it after the system fails to detect the lane marker (e.g., when false negatives arise or when no marker is present in the scene). In order to solve this specific problem, the FLane system employs the DMB module, as explained in Sec. 2.2.3. It is also worth mentioning that the knowledge of the pose of the lane marker in one image is used to determine the region of interest (ROI) to be processed for lane detection in the next frame. This makes the lane search more accurate and reduces computational requirement by eliminating much of the scene. Theoretical details of the FED, FLR, and DMB modules are presented in the remainder of this section.

2.2.1 Fuzzy Edge Detection. Hough transform is a commonly used technique to fit lines to detected edges. However, it typically suffers from heavy computational time and its performance largely depends on the result of the edge detection process. In order to apply effectively the Hough transform in real time and in a highly dynamic environment, the FLane system employs a fuzzy logic-based edge detection algorithm. The proposed approach is

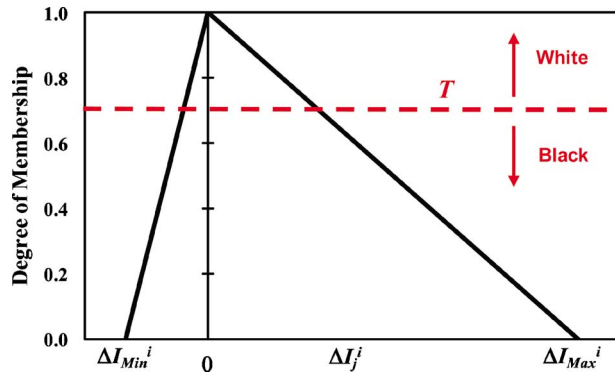


Fig. 5 Membership function of the intensity indicator. If the degree of membership is greater than a threshold T ($T=0.7$ in our case), then the pixel is accepted, and it is set to 1 (white), otherwise it is disregarded, and it is set to 0 (black).

intended to extract white lane markings regardless of variations in lighting conditions and road texture characteristics. It is suited to detect both solid and segmented lines. The basic idea of the FED module is that of extracting image points that satisfy two conditions: to have a specified gray level and to belong to a border region. To this end, a given pixel in the ROI is processed by what we define an intensity indicator (Ii) that estimates the likelihood that this pixel belongs to the lane model. The Ii compares the intensity level of the pixel with the average intensity value of the lane marker detected in the previous frame. Our hypothesis is that a large difference in intensity value suggests that the pixel does not belong to the model. We express this hypothesis using fuzzy logic. The triangular membership function used for the Ii, i.e., the curve that maps each point in the input space to a membership value or grade between zero and one, is shown in Fig. 5. The intensity indicator uses one input and one output. The input is the relative change in the intensity level of the pixel j of the ROI of image i with respect to the previous frame $i-1$ defined as

$$\Delta I_j^i = \frac{I_j^i - I_m^{i-1}}{I_m^{i-1}} \times 100 \quad (7)$$

where I_j^i is the intensity level of the pixel j of the frame i and I_m^{i-1} is the average intensity level of the lane marking detected in the frame $i-1$.

The output is a dimensionless factor ranging from zero to one that expresses the degree of confidence we have that the pixel j belongs to the model. It is important to notice that the performance of the FED module greatly depends on the value of the lower and upper limits of the triangular membership function, ΔI_{\min}^i and ΔI_{\max}^i , respectively, in Fig. 5. In the proposed implementation, ΔI_{\max}^i is well-experimentally determined as 90%, and ΔI_{\min}^i varies adaptively, depending on the average lighting change with respect to the previous frame. The details of the fuzzy-based regulation of the lower bound are included in Appendix for completeness.

A typical result of the thresholding using the Ii is shown in Fig. 6 for a sample image. Specifically, Fig. 6(a) shows the original image ROI. Figure 6(b) depicts the binary image obtained by the fuzzy thresholding, whereas Fig. 6(c) demonstrates the result of an independent Canny's edge detection [22]. Two binary images are available: one containing points whose gray level is similar to the gray level expected for the lane marker (Fig. 6(b)) and one containing strong edge points (Fig. 6(c)). A final binary image, suitable for Hough manipulation, can be obtained with a Boolean AND-operation, as shown in Fig. 6(d).

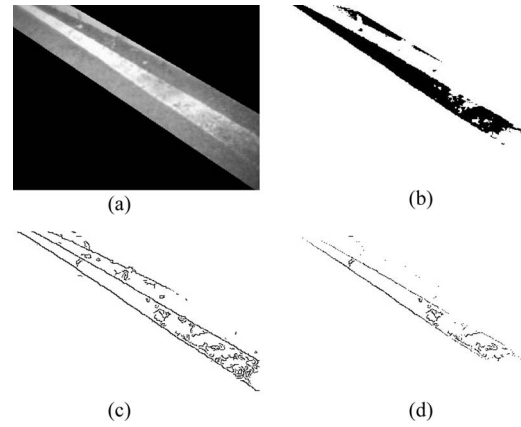


Fig. 6 Results of a sample image binarization using the fuzzy edge detection module: (a) selected ROI, (b) fuzzy thresholding using the Intensity Indicator, (c) Canny edge detection, and (d) Boolean AND of the two previous operations. Note that the negatives of the binary images are shown for visualization's sake.

One should note that relying only on the edge detection operator would have brought a more complex and uncertain thresholding of the scene, as apparent by comparing Fig. 6(d) with Fig. 6(c).

2.2.2 Fuzzy Lane Recognition. A set of lane candidates is made available by applying Hough transform to the output of the FED step. The FLR module allows the pair of lines that best agrees with the lane model to be selected. The general approach is based on comparing the geometrical properties of each candidate with those of the LM model in both the image plane and the real world and defining deterministic conditions for model matching. The output of the FLR module is a fuzzy quantity that expresses our certainty that the line pair matches the lane model. If n lines are detected in the image, then, there will be c lane marker candidates LM_j with $j=1, 2, \dots, c$, and

$$c = \frac{n!}{2!(n-2)!} \quad (8)$$

In the image plane, we can compute the pose $P_j^i = (\rho_j^i, \varphi_j^i)$ for each one of the lane marker candidates LM_j^i relative to frame i and compare this value with the pose of the lane marker obtained in the previous frame $P^{i-1} = (\rho^{i-1}, \varphi^{i-1})$. Under the assumption of a relatively small displacement of the vehicle with respect to the road marking between two consecutive frames, we can regard P^{i-1} as a good reference value. If the line pair pose P_j^i agrees with P^{i-1} , then one can expect good correspondence between that pair and the lane model. Poor correspondence suggests low likelihood of matching.

Similarly, we can compare the geometrical properties of the lane marker LM_j^i in the real world, i.e., W_j^i and the orientation θ_j^i , with the analogous parameters of the model obtained from the previous frame. A small difference in the values of width and orientation suggest high likelihood of matching of the candidate with the model. We again adopt fuzzy logic to express these hypotheses. The triangular membership functions of the inference system for the FLR module are shown in Fig. 7.

The fuzzy data fusion uses four inputs and one output. The inputs are the geometrical data, i.e., the absolute difference in distance and orientation estimated in the image plane, denoted with $\Delta \rho_j$ and $\Delta \varphi_j$, between the candidate pose and the model pose in the previous frame, and the absolute difference in width and orientation, denoted with ΔW_j and $\Delta \theta_j$, respectively, between the candidate and the model in the real world. The output is a dimensionless factor ranging from zero to one that expresses the degree of confidence we have that the line pair matches the lane model.

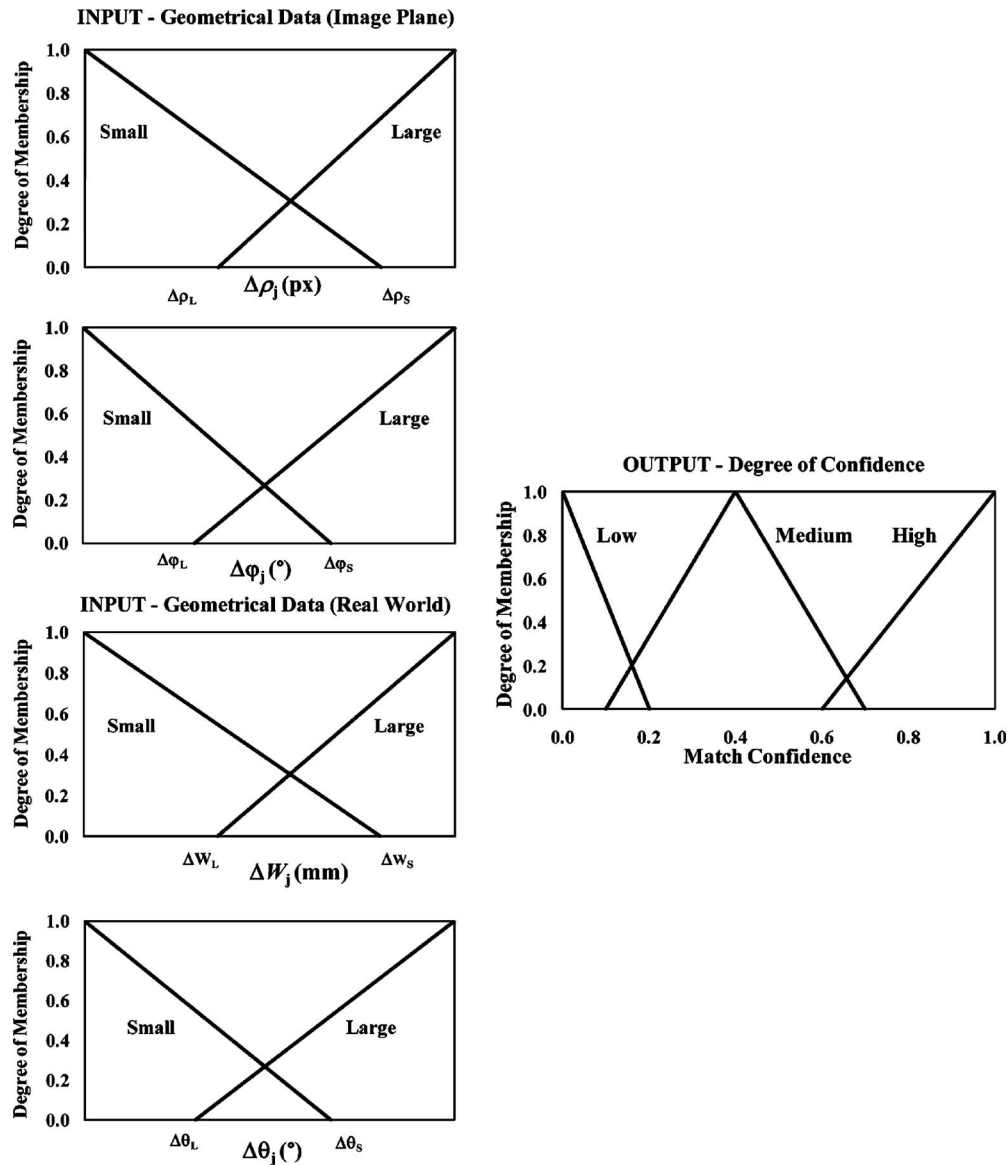


Fig. 7 Membership functions of the FLR module

The set of *if-then* rules used by the fuzzy inference system to fuse the geometrical information is shown in Table 1. Those rules express our physical understanding of the problem, and they were chosen to give the best performance over other alternatives using a trial and error process. The rule set is not unique; new rules may be thought of and implemented to improve the output of the system.

Table 1 Fuzzy logic rules used by the FLR module

Rule number	Input				Output
	$\Delta\rho_j$	$\Delta\phi_j$	ΔW_j	$\Delta\theta_j$	Match confidence
1	Small	Small	Small	Small	High
2	Small	Large	Small	Large	Medium
3	Large	Small	Large	Small	Low
4	Large	Large	Large	Large	Low
5	Large	Large	Small	Small	Low
6	Small	Small	Large	Large	Medium

The output of the FLR module is shown in Fig. 8 overlaid over the original scene of the running example of Fig. 6. Five lines are obtained by applying Hough transform; thus, ten lane marking candidates exist. Table 2 collects the match confidence estimated

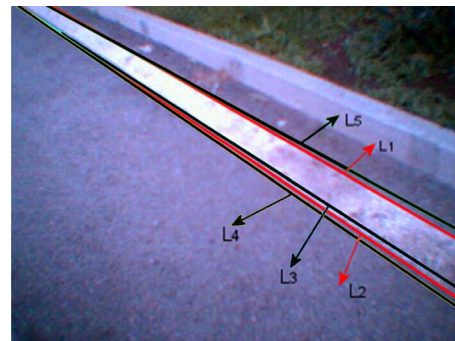


Fig. 8 Fuzzy lane selection applied to a sample image. Five lines were selected forming ten lane marker candidates.

Table 2 Degree of confidence for the lane marking candidates of Fig. 8, as derived by the FLR module

Candidate number	Lines involved	Match confidence (%)
1	L ₁ , L ₂	86.0
2	L ₁ , L ₃	77.0
3	L ₁ , L ₄	70.0
4	L ₁ , L ₅	3.4
5	L ₂ , L ₃	6.0
6	L ₂ , L ₄	6.2
7	L ₂ , L ₅	79.0
8	L ₃ , L ₄	5.7
9	L ₃ , L ₅	40.0
10	L ₄ , L ₅	40.1

by the FLR system for each candidate. As expected, the lane marker bounded by lines L₁ and L₂ (Fig. 8) yields the greatest confidence level (86.0%), and it is, therefore, selected as the best match.

It is worth noticing that the efficient filtering provided by the previous FED module (see Fig. 6(d)), allowed all the detected lines to be concentrated at the borders of the actual lane marker. The presence of multiple lines can be explained when considering the resolution of the Hough space. This makes the task for the FLR system relatively easy. However, this is not always the case. As an example, Fig. 9 shows a different scene where spurious road signs appear, resulting in a fictitious peak in the Hough space (due to line L₂ in Fig. 9(b)). Match confidences of the lane marker candidates for this case are reported in Table 3. All the stripes comprising the spurious line are labeled with low confidence by the FLR module and the lane model is correctly determined as the one formed by lines L₃ and L₄, with 82.1% of confidence, attesting to the feasibility of this approach.

Once the lane marker has been detected, the vehicle position and orientation relative to the lane can be estimated using inverse perspective projection [23], thus providing a valid input to vehicle-control and driver warning systems.

2.2.3 Dynamic Model Building. The accuracy of a lane detector greatly depends on the accuracy of the model adopted for the road marking. The best choice of road model is tightly connected with the environmental conditions in which the system is used. For example, a static model, built upon the initial geometrical and intensity properties of the road lane, could soon fail or give poor results because of changes in lighting conditions and lane marking shape or width during vehicle travel. The proposed DMB module allows the lane model to be built online following a multiframe approach by processing a short sequence of images (typically, from 10 to 20 frames, with less than 1 s period of time, are sufficient). It kicks in at the start of the lane detection operation or

Table 3 Degree of confidence for the lane marking candidates of Fig. 9 as derived by the FLR module

Candidate number	Lines involved	Match confidence (%)
1	L ₁ , L ₂	0.9
2	L ₁ , L ₃	3.2
3	L ₁ , L ₄	80.1
4	L ₁ , L ₅	3.3
5	L ₂ , L ₃	2.7
6	L ₂ , L ₄	7.8
7	L ₂ , L ₅	3.8
8	L ₃ , L ₄	82.1
9	L ₃ , L ₅	0.0
10	L ₄ , L ₅	40.0

when the system needs to update the model after failure. The only underlying assumption is that the vehicle is properly positioned on the road and that the lane marking is within the camera field of view.

In each frame of the sequence, the DMB module looks for the best model following a two-step approach. First, a Canny's edge detection is performed. Second, a bounded Hough transform is applied. Thus, a set of marker candidates j can be defined in terms of their parameters W_j and θ_j and compared with the nominal model to find the line pair that best satisfies constraints (5) and (6) for the given image. Fuzzy logic still represents a feasible and effective solution to this problem. Two inputs and one output are used in the fuzzy inference system, with the relative membership functions shown in Fig. 10.

The inputs (Fig. 10) are the absolute difference ΔW_j^0 between W_j and the nominal width \hat{W} and the absolute difference $\Delta \theta_j^0$ between θ_j and $\hat{\theta}$. The output expresses the match confidence of the lane marker j . The rules for the fuzzy inference engine are collected in Table 4, expressing the idea that the more the stripe is similar to the nominal model, the greater is the confidence that it actually represents the lane marker.

In order to combine robustly the results obtained from the single scenes of the sequence, a so-defined cumulative Hough matrix is proposed, whose conceptual scheme is shown in Fig. 11. For each image i , the computed model is added to the CHM, expressed in terms of coordinates of its border lines in the Hough space, namely, points (P_1^i, P_2^i) . After processing m frames, m lane marker candidates LM_i with $i=1, 2, \dots, m$, will be included in the CHM, distributed in cells, representing a small span of the Hough parameters. The larger the number of points falling into a given cell, the higher the likelihood that one of the two boundaries of the model belongs to this cell. Note that the vehicle's position and orientation with respect to the lane marking is assumed not to

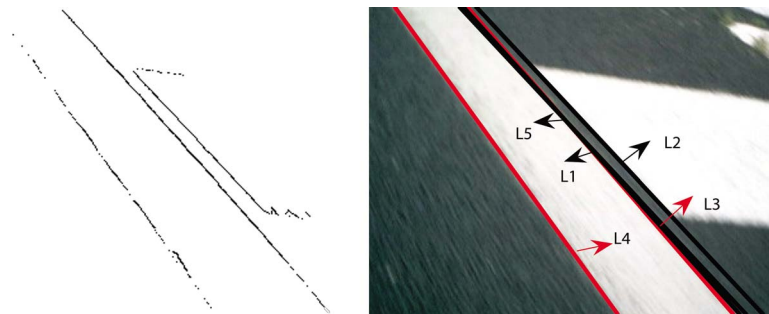


Fig. 9 Lane detection for a sample image where extraneous transversal white road markings are present: (a) output of the FED module and (b) indication of the lane marker candidates

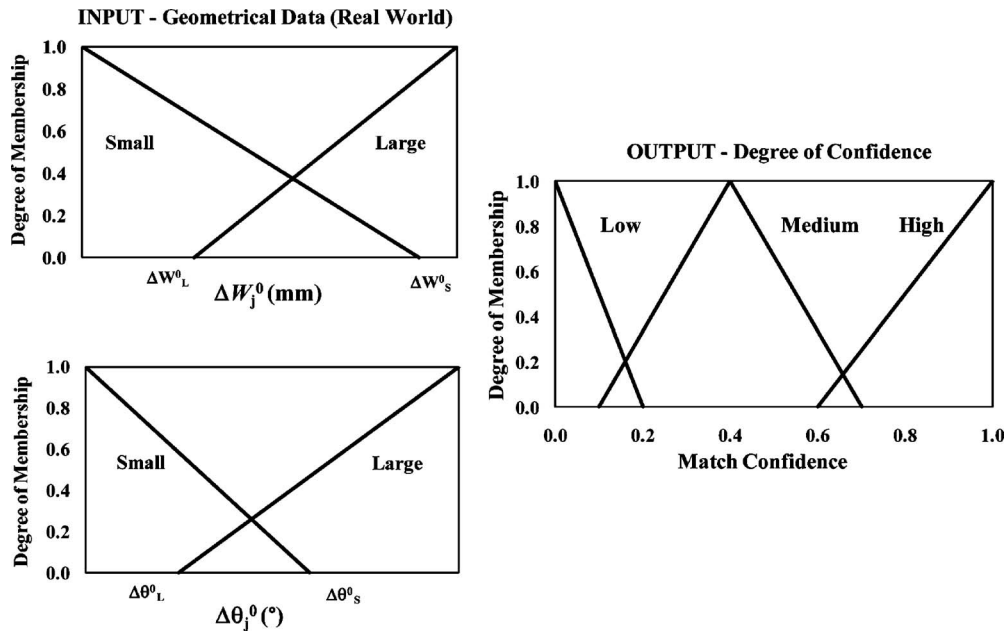


Fig. 10 DMB: input and output membership functions

change significantly during the model building stage. Eventually, the two cells with the largest number of points are selected (cells denoted by a dashed rectangle in Fig. 11), and the last points added to these cells (denoted with P_1^K and P_2^K in Fig. 11), are chosen as the best-updated estimate of the model.

Once the lane marker has been identified, its geometrical properties are known in both the image plane and the real world. In addition, the appearance properties of the marker, i.e., the average intensity of the pixels bounded by the two lines, can also be determined. All the estimated properties of the lane marker are passed on to the FLane tracking system that can start its tracking task. Representative results obtained from the DMB module are shown in Fig. 12 for a sample set of ten frames, acquired in a 0.5

s window, with the vehicle moving at about 40 km/h. Specifically, Figs. 12(a) and 12(b) show frames #1 and #5 of the sequence, with the overlaid selected lane marker and the assigned confidence level. Figure 12(c) illustrates the CHM for the test sequence.

The two cells with the largest number of points originate two peaks in the CHM, corresponding to the lane marker borders depicted in Fig. 12(d). Note that, in this example, the lane marker was properly identified in every frame of the sequence, and the border lines have their corresponding Hough points concentrated in only two cells of the CHM. However, it may occur that either the marker is not detected or misidentifications arise in one or more frames due to bad illumination conditions, wide occlusions, presence of multiple white stripes, or even absence of the marker. In such a case, the use of multiple frames helps to keep a robust estimation of the model, as demonstrated by the sequence shown in Fig. 13.

Finally, one should note that the reliability of the DMB output can be assessed by evaluating the score assigned to the lane model, and the process can be possibly repeated until a sufficiently high-confidence model is achieved.

Table 4 Fuzzy logic rules used by the DMB

Rule number	Input		Output
	ΔW_j^0	$\Delta \theta_j^0$	Match confidence
1	Small	Small	High
2	Small	Large	Medium
3	Large	Small	Medium
4	Large	Large	Low

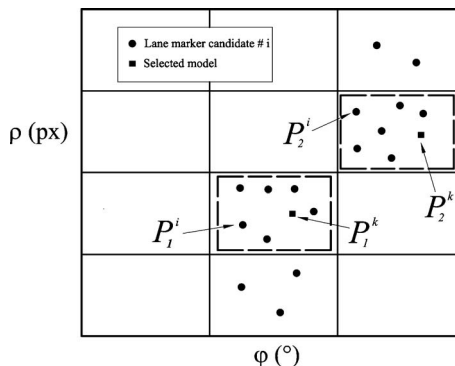


Fig. 11 Conceptual scheme of the CHM

3 Experimental Results

In this section, we present a comprehensive set of experiments to validate our approach. The FLane system was tested in the field on a commercial automobile, as shown in Fig. 14. A C++ compiled implementation of the algorithm processed images in real time at 20 Hz on a 1.86 GHz Pentium III-M laptop. The executable version of the code required 120 KB of memory for the program, with an additional 225 KB of memory for execution. These low requirements suggest that the algorithm is suitable for on-board implementation with limited computational resources. Additionally, a cost-effective webcam, mounted sideways, was used for image acquisition to demonstrate the effectiveness of the algorithm with poor hardware resource. The webcam was calibrated using the MATLAB camera calibration toolbox [24]. Data were collected from portions of four kinds of roads at different times of the day. Details are given in Table 5. Sequence A refers to urban road with solid or dotted lane markings and heavy disturbances due to curbs, manhole covers, etc. Typical freeway conditions with solid or dotted road markings and complex shadowing

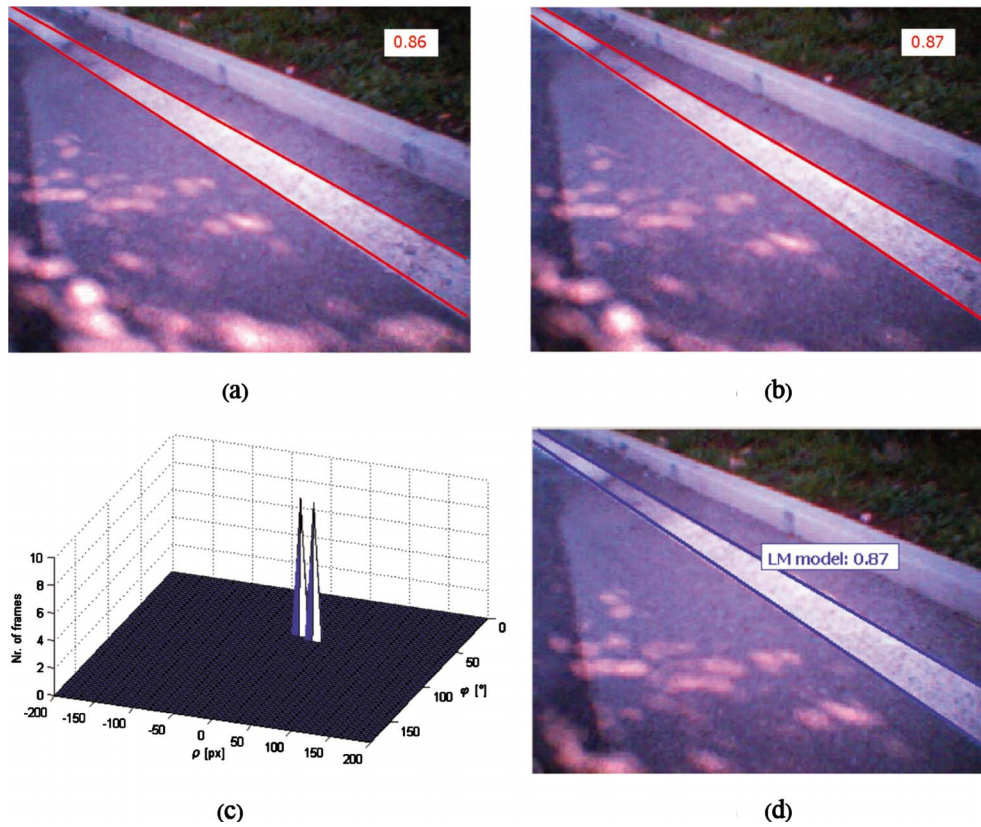


Fig. 12 Result of the DMB module applied to a sample sequence: (a) first frame of the sequence, (b) fifth frame of the sequence, (c) representation of the CHM, and (d) selected lane marker model. Images (a) and (b) report indication of the confidence assigned to the selected lane marker.

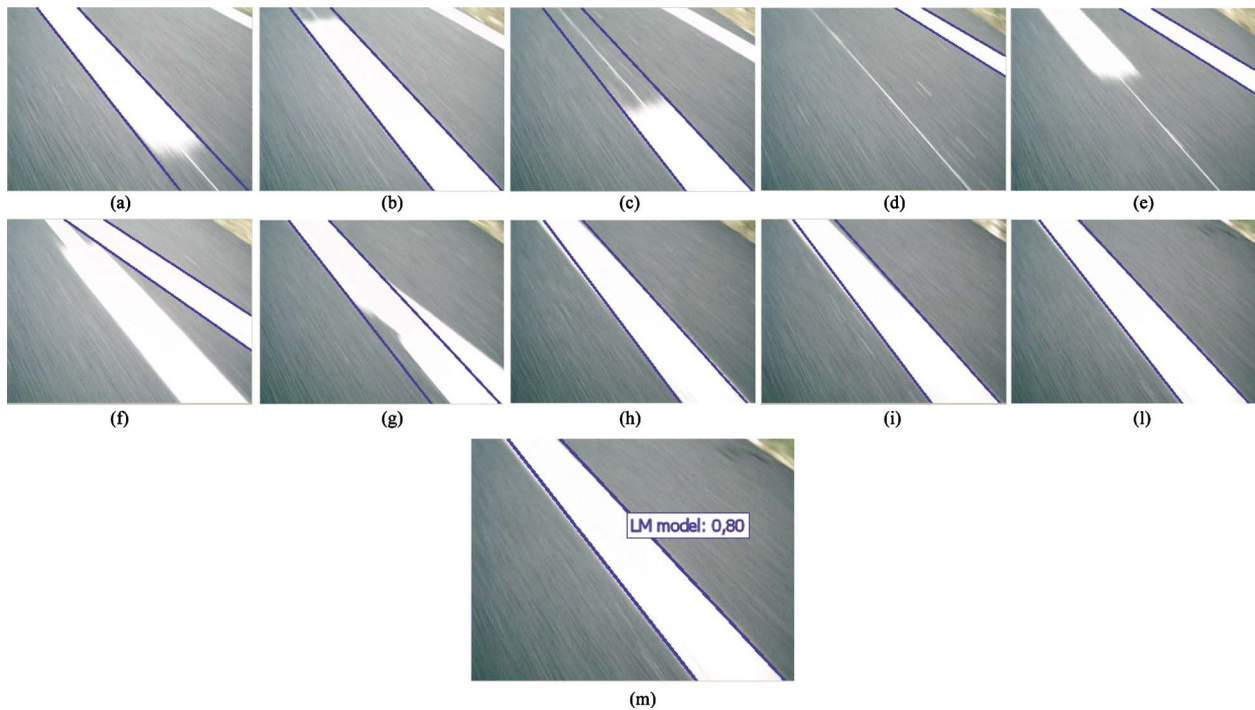


Fig. 13 Example of robust marker model building: (a)-(l) consecutive frames used for model building; (m) marker model obtained as output of the DMB module. Although the absence of the main lane marker in (d) or the presence of multiple lines in (e), (f) and results in misidentifications, the DMB module retains a correct model.



Fig. 14 The test bed used for experimental validation of the FLane system

due to overpasses and other cars and changes in road surface material are shown in sequences B, C, and D at different times of the day: noon, dusk, and night, respectively. The FLane system was tested over a total of 44,850 frames (approximately 35 km of total travel distance), showing the results summarized in Table 6.

The percentage of false positives, false negatives, and misidentifications is shown for each image set. False positives occur when a lane marker is recognized when actually there is no lane marking. This is due to spurious objects in the scene, which somehow match the lane model. As an example, Fig. 15 shows a scene where the FLane system erroneously detected a lane marker, misled by the grids of a manhole cover. In our tests, the percentage of false positives was always less than 3%. Conversely, false nega-

Table 5 Set of sequences showing the environmental variability caused by road markings and surfaces and lighting

Set	Road	Road marking	Day time
A	Urban and rural	Solid or dotted lines	Noon
		Occlusions and disturbances Low contrast between road texture and line	
B	Highway	Solid or dotted lines	Noon
C	Highway	Solid or dotted lines	Dusk
D	Highway	Solid lines	Night

Table 6 Performance of the FLane system under various lighting and road conditions

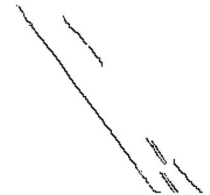
Set	Frames	False positives (%)	False negatives (%)	Misid. (%)
A	10,450	2.8	5.6	2.5
B	15,400	0.0	3.7	0.0
C	11,460	0.0	1.5	0.5
D	7,540	1.4	0.5	0.6



(a)



(a)



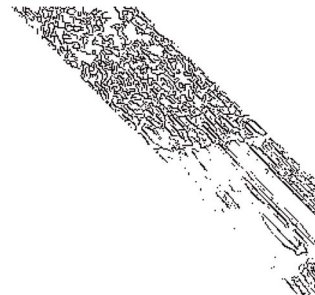
(b)

Fig. 16 Example of false negative due to poor image segmentation: (a) black lines: lane candidates; and (b) output of the FED module.

tives arise when the lane marker is present in the image but the system is not able to detect it at all, and it does not return any information. The percentage of false negatives was less than 6% and due mainly to partially-deleted road marking, poor image segmentation, and camera calibration errors, as shown by the example of Fig. 16, where the FLane system failed. However, we should emphasize that this type of error may be greatly mitigated by adopting a more sophisticated hardware set. Finally, misidentifications refer to cases in which a lane marker is present in the image but the system fails in recognizing it properly and returns wrong information. In all tests, misidentifications were less than 3%. As expected, set A presented error rates greater than sets B, C, and D.

Table 7 shows some typical results for sample images extracted from each one of the sequences investigated. The initial model of the lane marker was constructed online with our DMB approach employing a set of ten frames. The initial models are also shown in the first column of Table 7 with overlaid the confidence level. Finally, Table 8 collects the output of the FLane system for particularly challenging situations. Specifically, the images extracted from sequence A refer to two scenarios characterized by high level of noise, low contrast between road texture and lane marker, and sudden lighting variations. Although the application of the FED module resulted in the detection of multiple spurious lines (denoted by black lines) due to poor image segmentation, the FLR module correctly identified the lane marker (grey lines or red lines in the online version of the paper). The images from set D also confirm the effectiveness of the proposed approach in very poor lighting conditions and in presence of multiple reflections and shadows.

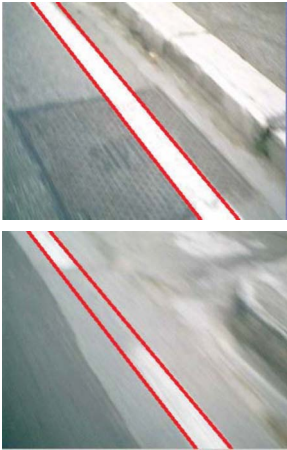
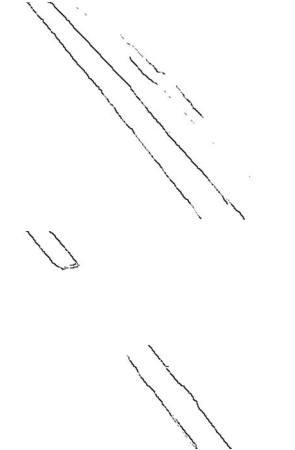
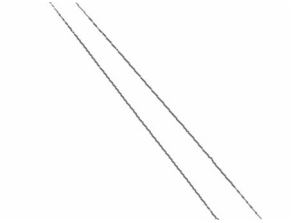
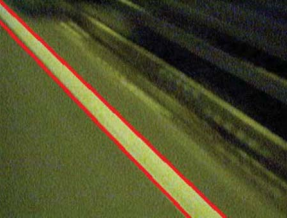
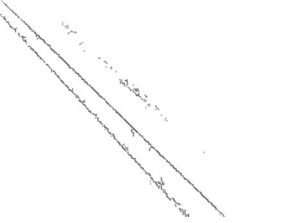
In conclusion, the FLane system proved effective in field testing providing a fast measurement update every few meters of



(b)

Fig. 15 Example of false positive due the presence of a manhole cover: (a) grey lines (red lines in the online version of the paper): erroneous lane marker estimated by the FLane system and black lines: lane candidates; and (b) output of the FED module

Table 7 Typical results obtained from the FLane system for different environmental conditions, as described in Table 5. Please refer to Secs. 2.2.1 and 2.2.2 for more details on the image processing.

SET	DMB	FLane	Fuzzy Edge Detection
A			
B			
C			
D			

travel distance (e.g., 1.4 m at a speed of 100 km/h) that enforced the small variation assumption adopted for the lane model.

4 Conclusions

In this paper, we presented a method for detecting and tracking lateral lane markings in real time and in a highly dynamic environment, referred to as fuzzy logic lane tracking system. The FLane system uses Hough transform in conjunction with fuzzy reasoning to provide high flexibility and ability to adapt to different roads and environmental conditions. Experimental results, obtained with our system integrated with a commercial automobile, and using a cost-effective webcam showed the feasibility of our approach and its robustness to variations in lighting and road conditions, with a worst-case of less than 6% of failed observations in urban roads. It was shown that the FLane module could be effectively employed in the development of autonomous vehicles and driver assistance systems.

Appendix

If we introduce an average relative intensity variation between the ROI of two consecutive frames i and $i-1$ as

$$\Delta I_{\text{ROI}}^i = \left(\frac{I_{\text{ROI}}^i - I_{\text{ROI}}^{i-1}}{I_{\text{ROI}}^{i-1}} \right) \times 100 \quad (\text{A1})$$

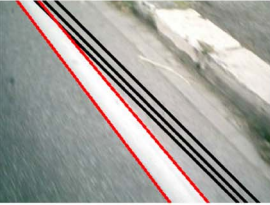
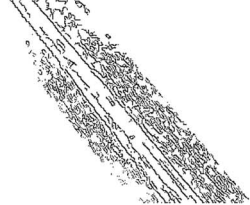
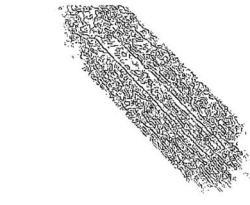
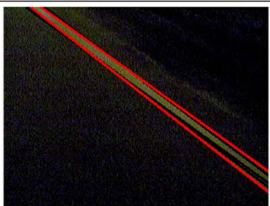
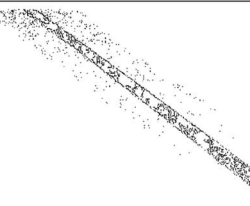
where I_{ROI}^i is the average intensity value within the ROI of frame i and I_{ROI}^{i-1} is the average intensity value within the ROI of frame $i-1$.

Then, we can define ΔI_{min}^i as

$$\Delta I_{\text{min}}^i = \Delta I_{\text{min}}^{i-1} + k_i \cdot \Delta I_{\text{ROI}}^i \quad (\text{A2})$$

with k_i being a weighting factor, which depends on the value of ΔI_{ROI}^i . For a finer gradation, we also express this relationship with fuzzy logic. The input to the fuzzy inference system is the value of ΔI_{ROI}^i and the output is the gain k_i ranging from zero to one.

Table 8 Results obtained from the FLane system in challenging situations encountered in set A (urban and rural road) and D (night-time acquisition). Candidate lines are shown in black; grey (red) lines indicate the selected lane marker.

SET	FLane	Fuzzy Edge Detection
A		
		
D		
		

References

[1] McCall, J. C., and Trivedi, M. M., 2006, "Video-Based Lane Estimation and Tracking for Driver Assistance: Survey, System, and Evaluation," *IEEE Trans. Intell. Transp. Syst.*, **7**(1), pp. 20–37.

[2] Godthelp, H., Milgram, P., and Blaauw, G. J., 1984, "The Development of a Time Related Measure to Describe Driving Strategy," *Hum. Factors*, **26**, pp. 257–268.

[3] McCall, J., and Trivedi, M. M., 2004, "Visual Context Capture and Analysis for Driver Attention Monitoring," *Proceedings of the IEEE Conference on Intelligent Transportation Systems*, Washington, DC, pp. 332–337.

[4] Taylor, C., Košecká, J., Blasi, R., and Malik, J., 1999, "A Comparative Study of Vision-Based Lateral Control Strategies for Autonomous Highway Driving," *Int. J. Robot. Res.*, **18**(5), pp. 442–453.

[5] Hough, P., 1962, "Methods and Means for Recognizing Complex Patterns," U.S. Patent No. 3069654.

[6] McDonald, J., 2001, "Detecting and Tracking Road Markings Using the Hough Transform," *Proceedings of the Conference of the Irish Machine Vision and Image Processing*, Maynooth, Ireland, pp. 1–9.

[7] Pomerleau, D., 1995, "RALPH: Rapidly Adapting Lateral Position Handler," *Proceedings of the IEEE Symposium on Intelligent Vehicles*, Detroit, MI, pp. 506–511.

[8] Furusho, H., Shirato, R., and Shimakage, M. A., 2002, "Lane Recognition Method Using the Tangent Vectors of White Lane Markers," *Proceedings of the International Symposium on Advanced Vehicle Control*, pp. 1–6.

[9] Gehrig, S., Germ, A., Heinrich, S., and Woltermann, B., 2002, "Lane Recognition on poorly Structured Roads—The Bot Dot Problem in California," *Proceedings of the Conference on Intelligent Transportation Systems*, pp. 67–71.

[10] Southall, J. B., and Taylor, C. J., 2001, "Stochastic Road Shape Estimation," *Proceedings of the Conference on Computer Vision*, Vancouver, Canada, pp. 205–212.

[11] Kim, Z. W., 2008, "Robust Lane Detection and Tracking in Challenging Scenarios," *IEEE Trans. Intell. Transp. Syst.*, **9**(1), pp. 16–26.

[12] Danescu, R., and Nedevschi, S., 2009, "Probabilistic Lane Tracking in Difficult Road Scenarios Using Stereovision," *IEEE Trans. Intell. Transp. Syst.*, **10**(2), pp. 272–282.

[13] Bertozzi, M., and Broggi, A., 1998, "GOLD: A Parallel Real-Time Stereo Vision System for Generic Obstacle and Lane Detection," *IEEE Trans. Image Process.*, **7**(1), pp. 62–81.

[14] McCall, J., and Trivedi, M., 2005, "Performance Evaluation of a Vision Based Lane Tracker Designed for Driver Assistance Systems," *Proceedings of the IEEE Symposium on International Vehicles*, pp. 153–158.

[15] Kreucher, C., and Lakshmanan, S., 1999, "LANA: A Lane Extraction Algorithm That Uses Frequency Domain Features," *IEEE Trans. Rob. Autom.*, **15**(2), pp. 343–350.

[16] Pomerleau, D.; Jochem, T., 1996, "Rapidly Adapting Machine Vision for Automated Vehicle Steering," *IEEE Expert*, **11**(2), pp. 19–27.

[17] Mendel, J. M., 1995, "Fuzzy Logic Systems for Engineering: A Tutorial," *Proc. IEEE*, **83**(3), pp. 345–377.

[18] Siler, W., and Buckley, J. J., 2005, "Fuzzy Expert and Fuzzy Reasoning," Wiley, New Jersey.

[19] Russo, F., and Ramponi, G., 1994, "Edge Extraction by FIRE Operators," *Proceedings of the IEEE International Conference on Fuzzy Systems*, pp. 1143–1146.

[20] Wei Li, G. T., and Wang, Y., 1997, "Recognizing White Line Markings for Vision-Guided Vehicle Navigation by Fuzzy Reasoning," *Pattern Recogn. Lett.*, **18**(8), pp. 771–780.

[21] Reina, G., and Yoshida, K., 2008, "Estimation for Lunar and Planetary Robots," *Int. J. Intell. Contr. Syst.*, **13**(1), pp. 15–24.

[22] Canny, J., 1986, "A Computational Approach to Edge Detection," *IEEE Trans. Pattern Anal. Mach. Intell.*, **PAMI-8**(6), pp. 679–698.

[23] Milella, A., Venturino, L., Gramegna, T., and Cicirelli, G., 2004, "Robot Localization and Path Following Based on Detection of Visual Structures," *Proceedings of the IEEE International Conference on Mechatronics and Machine Vision in Practice*, pp. 16–23.

[24] Bouguet, J., *Camera Calibration Toolbox for MATLAB*, 2004, available online at http://www.vision.caltech.edu/bouguetj/calib_doc/